Biogeosciences Discuss., https://doi.org/10.5194/bg-2017-481
Manuscript under review for journal Biogeosciences
Discussion started: 11 December 2017

Biogeosciences Discussions Open Access EGU

Impact of salinity on element incorporation in two benthic foraminiferal species with contrasting Magnesium contents

Esmee Geerken[1], Lennart Jan de Nooijer[1], Inge van Dijk[1,2] & Gert-Jan Reichart[1,3]

[1]Department of Ocean Systems, NIOZ-Royal Netherlands Institute for Sea Research, and Utrecht University, Den Burg, The Netherlands

[2]Currently at: UMR CNRS 6112 LPG-BIAF, Bio-Indicateurs Actuels et Fossiles, Angers University, France

[3]Faculty of Geosciences, Utrecht University, Utrecht, The Netherlands

Correspondence to: Esmee Geerken (esmee.geerken@nioz.nl)

Abstract. Accurate reconstructions of seawater salinity could provide valuable constraints for studying past ocean circulation, the hydrological cycle and sea level change. Controlled growth experiments and field studies have shown the potential of foraminiferal Na/Ca as a direct salinity proxy. Incorporation of minor and trace elements in foraminiferal shell carbonate varies, however, greatly between species and hence extrapolating calibrations to other species needs validation by additional (culturing) studies. Salinity is also known to impact other foraminiferal carbonate-based proxies, such as Mg/Ca for temperature and Sr/Ca for seawater carbonate chemistry. Better constraints on the role of salinity on these proxies will improve their reliability. Using a controlled growth experiment spanning a salinity range of 20 units and analysis of single chamber element composition using laser ablation-ICP-MS, we here show that Na/Ca correlates positively with salinity in two benthic foraminiferal species (*Ammonia tepida* and *Amphistegina lessonii*). The Na/Ca values differ between the two species, with an approximately 2-fold higher Na/Ca in *Amphistegina* than in *Ammonia*, which coincides with an offset in their Mg content (~35 mmol/mol versus ~2.5 mmol/mol for *A. lessonii* and *A. tepida*, respectively). Despite the offset in average Na/Ca values, the slopes of the Na/Ca-salinity regressions are similar between these two species. In addition, Mg/Ca and Sr/Ca are positively correlated with salinity in cultured *A. tepida*, but do not show a correlation to salinity for *A. lessonii*. Electron microprobe mapping of incorporated Na and Mg of the cultured specimens shows that within chamber walls of *A. lessonii*, Na/Ca and Mg/Ca occur in elevated bands in close proximity to the primary organic lining. For specimens of *A. tepida*, Mg-banding shows a similar pattern to that in *A. lessonii*, albeit that variation within the chamber wall is much less pronounced. Also Na-banding is much less prominent in this species. The less prominent banding and lower Mg and Sr contents of *A. tepida* are likely related to the absence of an inter-element correlation within experimental conditions.

Biogeosciences Discuss., https://doi.org/10.5194/bg-2017-481
Manuscript under review for journal Biogeosciences
Discussion started: 11 December 2017

1. Introduction

Seawater salinity varies over time and space as a function of continental ice volume, evaporation, precipitation and river runoff. Reconstructions of salinity could provide important constraints on past ocean circulation, the hydrological cycle and glacial-interglacial sea level changes. Currently, most reconstructions of salinity are indirect and based on the correlation between salinity and $\delta^{18}O_{water}$, assuming this relationship to be constant over space and time. An independent salinity proxy may reduce the uncertainties inherently associated with such approaches and should preferably be based on one of the main components of seawater salinity, for instance sodium (Na). Results from a culture study showed that foraminiferal calcitic Na/Ca (Na/Ca_{cc}) correlates positively and linearly with salinity for the low-Mg benthic symbiont-barren species *Ammonia tepida*, with a slope of 0.22 between salinities 30 and 38.6 (Wit et al., 2013). Various culture studies earlier showed that also Mg/Ca is affected by salinity, but respond more strongly to temperature (Lea et al., 1999; Dissard et al., 2010b; Nürnberg et al., 1996; Hönisch et al., 2013). Although an effect of salinity on foraminiferal Sr/Ca_{cc} has been reported in some studies (Kısakürek et al., 2008; Dissard et al., 2010b; Wit et al., 2013) other studies did not find a relation between salinity and foraminiferal Sr/Ca (Dueñas-Bohórquez et al., 2009; Diz et al., 2012; Allen et al., 2016) which is thought to mainly reflect sea water carbonate chemistry (Keul et al., 2017) and temperature (Nürnberg et al., 1996; Lea et al., 1999; Raja et al., 2007). Hence, an independent salinity proxy would not only be useful for constraining past (changes in) salinity, but also improve temperature reconstructions based on Mg/Ca_{cc} and reconstructions of past sea water carbonate chemistry based on Sr/Ca.

Following the culture-based Na/Ca_{cc}-salinity calibration for *A. tepida* (Wit et al., 2013), a culture study with planktonic symbiont-bearing species also showed a significant linear relationship for *Globigerinoides ruber (Allen et al., 2016).* Although no significant relationship was observed in this study for *G. sacculifer* (Allen et al., 2016), a recent field calibration observed positive linear relationships for both species (Mezger et al., 2016). Still, the Na/Ca-salinity sensitivities observed between the different species and studies differed considerably (ranging from a change in 0.074 to 0.66 mmol/mol in Na/Ca_{cc} for a change in 1 salinity unit). Whereas Wit et al. (2013) suggested an incorporation mechanism similar to that observed in inorganic calcite, field and culture studies also show that different species of foraminifera have varying calcite chemistries, thereby resulting in the need of species-specific calibrations similar to many other foraminiferal trace metal-based proxies (e.g. Elderfield and Ganssen, 2000; Rosenthal et al., 2000; Anand et al., 2003; Bemis et al., 1998; Toyofuku et al., 2011). Mg/Ca_{cc} values for example are different between groups of low-Mg-, high-Mg hyaline and porcelaneous foraminifera (Toyofuku et al., 2000; Segev and Erez, 2006; Raja et al., 2007), which also seems to be reflected in other co-precipitated cations (De Nooijer et al., 2017). Hence, calibration of Na/Ca_{cc} as a function of salinity for other species is not only necessary to test the applicability of this novel proxy for other groups of foraminifera, but also allows testing whether monovalent cations follow the inter-species trends described for divalent cations (Terakado et al., 2010).

Here we calibrated Na-, Mg- and Sr-incorporation in the intermediate-Mg calcite, benthic symbiont-bearing, tropical foraminifer *Amphistegina lessonii* and the low-Mg calcite, symbiont-barren, intertidal species *Ammonia tepida* over a salinity range of 20 units (from 25 to 45) and compare obtained ratios

with existing calibrations. The chemical composition of the calcite was determined by Laser Ablation Inductively Coupled Plasma Mass Spectrometry (LA-ICP-MS), providing insights in concentrations and variability in concentrations between specimens and between single chambers. To investigate intra-specimen variability at the scale of the chamber wall we also performed Electron Probe Micro Analysis (EPMA), mapping the Ca, Na and Mg distribution throughout the chamber wall for specimens of both species cultured.

2. Methods

2.1 Collection of foraminifera and culture set-up

Surface sediment samples containing foraminifera (*A. lessonii*) were collected from the Indo-Pacific Coral Reef aquarium in Burgers' Zoo (Arnhem, The Netherlands; Ernst et al., 2011) and a tidal flat near Den Oever, the Wadden Sea (*A. tepida*). Sediment was stored in aerated aquaria at 25°C (*A. lessonii*) and 10°C (*A. tepida*) with a day/night cycle of 12/12 hours, similar to conditions in the coral reef aquarium and Wadden Sea. From both stocks, living specimens, recognized by chambers that were filled with yellow cytoplasm and pseudopodial activity, were isolated.

Living specimens were placed in groups of 25 individuals in Petri dishes with approximately 70 ml of North Atlantic surface seawater (0.2 µm filtered) and fed with fresh cells of the algae *Dunaliella salina*. After reproduction, which occurred in approximately 2/3 of all incubated specimens, 2-3 chambered juveniles were isolated (De Nooijer et al., 2014). The use of specimens from reproduction events guarantees that virtually all chambers present at the end of the experiment were produced under the culture conditions (De Nooijer et al., 2014). Strains of specimens of the reproduction events (2-10 individuals) were divided over Petri dishes with approximately 10 ml culture medium and stored in a temperature controlled incubator set at 25 °C with a day/night cycle of 12/12 hours. The culture media in the Petri dishes were replaced once every week, after which specimens were fed with approximately 1 ml concentrated and freeze-dried *Dunaliella salina* diluted with the culture medium for each salinity to avoid changes in salinity. After 6-8 weeks, specimens were harvested and transferred to microvials to clean the specimens' carbonate shells from cell material. Organic matter was removed by adding 70% H_2O_2 buffered with 0.1M NH_4OH at 90 °C and gentle ultrasonication for 1 min. Specimens were subsequently rinsed 3 times with double deionized water, dried in a laminar flow cabinet, after which their size was determined (i.e. the maximum diameter crossing the center of the specimen). The specimens were thereafter stored until geochemical analyses (LA-ICP-MS; 2.2.2 and EPMA; 2.4).

2.2 Analytical methods

2.2.1 Culture media preparation and chemistry

In total, 50 L of seawater with a salinity of 50 was prepared by sub-boiling 0.2 µm filtered North Atlantic seawater for 48 hours at 45 °C. Subsequently, culture media were obtained by diluting this high-saline seawater with double de-ionized seawater in batches of approximately 10L with salinity

Biogeosciences Discuss., https://doi.org/10.5194/bg-2017-481
Manuscript under review for journal Biogeosciences
Discussion started: 11 December 2017

increasing from 25 to 45 in steps of 5 units, resulting in 5 unique salinity conditions. Using a single batch of concentrated seawater to subsequently dilute to the desired salinities ensures constant element to Ca ratios. Culture media were stored in Nalgene containers and kept in the dark at 10 °C. Seawater pH was determined with a pH meter (pH110, VWR). Subsamples were taken prior to and at the end of the experiment and analyzed for DIC and element concentrations to monitor the effect of sub-boiling on the seawater's inorganic carbon chemistry and element composition (Table 1). Subsamples for DIC were collected in headspace-free vials and conserved with a saturated $HgCl_2$ solution (10µl $HgCl_2$/10 ml sample). DIC measurements were performed on an autoanalyzer spectrometric system (TRAACS 800; (Stoll et al., 2001). This analysis requires only a small amount of sample, while yielding high accuracy (±2 µmol/kg) and precision (±1.5 µmol/kg). The minor and major elemental composition of the culture media was measured using a sector field ICP-MS (Element2, Thermo Scientific) by sampling 1 ml from the culture media and dilution by a factor 300 with0.14 M HNO_3 (Table 1).

Table 1. Experiment culture media measurements per salinity condition.

Experiment	Na/Ca_{sw} mol/mol	Mg/Ca_{sw} mol/mol	Sr/Ca_{sw} mmol/mol	Salinity	DIC µmol/kg	pH	$[CO_3^{2-}]$ mmol/kgSW	ΩCa
S25	48.84	5.61	9.37	25.2	1087.3	8.32	164.90	4.28
S30	49.79	5.69	9.45	30.3	1305.3	8.28	205.98	5.15
S35	48.56	5.51	9.04	35.2	1512.0	8.22	258.84	6.22
S40	48.50	5.62	9.19	40.0	1734.4	8.17	267.23	6.16
S45	48.90	5.73	9.21	45.2	1947.4	8.10	284.67	6.23

2.2.2 Foraminiferal calcite chemistry

Specimens were fixed on a laser ablation-stub using double sided tape, carefully positioning them to allow ablation of the last chambers (Appendix A). Element concentrations of individual chambers were measured with LA-ICP-MS (Reichart et al., 2003). The last 1-3 chambers of each specimen were ablated using a circular spot with a diameter of 80 µm (NWR193UC, New Wave Research) in a helium environment in a New Wave TV2 dual-volume cell (cup volume of ~1 cm^3) at a repetition rate of 6 Hz and an energy density of approximately 1 J/cm^2. The aerosol was transported to a quadrupole ICP-MS (iCap, Thermo Scientific) on a helium flow at a rate of 0.7 L/min, with 0.4 L/min Argon make-up gas being added before entering the torch. Monitored masses included ^{23}Na, ^{24}Mg, ^{25}Mg, ^{27}Al, ^{43}Ca, ^{44}Ca, ^{55}Mn, ^{88}Sr and ^{137}Ba, with one full cycle through the different masses taking 90 ms. Calibration was performed against a MACS-3 (synthetic calcium carbonate) pressed powder carbonate standard with ^{43}Ca as an internal standard. Count rates for the different masses were directly translated into element/Ca_{cc} (El/Ca_{cc}) ratios. Internal precision based on MACS-3 is 4% for Na, 3% for Mg and 4% for Sr. Accuracy and relative analytical errors, based on measuring international standards JCp-1 coral (*Porites* sp.) powder and the NIST (National Institute of Standards and Technology) SRM 610 and SRM 612 (glass) are listed in Table 2. The relatively large offset between the glass standards and the pressed powders (both MACS-3 and JCp-1) is known not to influence obtained El/Ca_{cc} ratios when either one is used as calibration standard (Hathorne et al., 2008), but due to the similar matrix, MACS-3 was chosen as calibration standard.

Biogeosciences Discuss., https://doi.org/10.5194/bg-2017-481
Manuscript under review for journal Biogeosciences
Discussion started: 11 December 2017

142 **Table 2.** Accuracies and precisions for Na, Mg and Sr for the various standards analyzed.

Standard	n	Accuracy Na (%)	Precision Na (%)	Ac Mg (%)	Pr Mg (%)	Ac Sr (%)	Pr Sr (%)
JCp-1	51	99	6	96	6	96	4
NIST610	32	119	3	104	2	110	3
NIST612	29	119	3	104	2	110	2

143

144 In total, 675 chambers were measured (336 for *Amphistegina* and 339 for *Ammonia*), resulting in
145 between 52 to 125 single chamber measurements per salinity condition per species. These
146 measurements were done on the last three (final or F, penultimate or F-1 and F-2) chambers of these
147 specimens. For *Amphistegina*, these chambers were derived from (condition/no of specimens/average
148 spots per specimen): S25/28/2.6, S30/40/1.9, S35/60/1.9, S40/27/2 and S45/33/1.4. For *Ammonia*, the
149 number of analyses were (condition/ no of specimens/ average spots per specimen): S25/44/2.5,
150 S30/31/1.8, S35/33/1.8, S40/52/1.8, S45/15/1.3. Element concentrations were calculated from the time
151 (i.e. ablation depth) resolved profiles using an adapted version (for details see Van Dijk et al., 2017a)
152 of the SILLS (Signal Integration for Laboratory Laser Systems; Guillong et al., 2008)) package for
153 MATLAB, while taking care to exclude contaminations potentially present on chamber walls
154 (examples of profile selection: Duenas-Bohorquez et al., 2011; Wit et al., 2013; Mewes et al., 2014;
155 Mezger et al., 2016; Van Dijk et al., 2017b). Measurements with ablation yields or integrations times
156 <5 s were excluded from further analysis.
157 Since there is variability in Ca counts between the laser ablation measurements, single-spot based
158 Element/Ca_{cc} ratios may cause spurious correlation due to coupled differences in Ca counts. To test
159 whether observed correlations between Na/Ca_{cc}, Sr/Ca_{cc} and Mg/Ca_{cc}, based on single-spots, are due to
160 the use of a common denominator (Ca), we performed a Monte Carlo simulation. In short, the
161 correlation coefficients between randomly drawn single-spot Mg concentration, divided by measured
162 Ca, and measured Na/Ca_{cc} concentrations were compared to the correlation coefficient of measured
163 Na/Ca_{cc} and Mg/Ca_{cc} concentration ratios in our dataset. By using a Kernel fit of the measured data set
164 to draw the random data set and using the measured Ca as a common denominator we effectively
165 simulate the spurious correlation. This was repeated 10,000 times and repeated for the couples
166 Mg/Ca_{cc}-Sr/Ca_{cc} and Na/Ca_{cc}-Sr/Ca_{cc} (Appendix B).
167 Furthermore, to test whether Sr/Ca_{cc} and Na/Ca_{cc} variability in *A. lessonii* is not caused by variability in
168 Mg content due to a potential closed sum effect (since high amounts of incorporated Mg cations could
169 reduce the Ca content of the shell and hence result in apparently elevated Sr/Ca_{cc} and Na/Ca_{cc}), we
170 calculated maximum variability due to the sole effect of Mg-substitution. For *A. lessonii*, variability
171 (standard deviation) of ±0.09 mmol/mol in Na/Ca_{cc} and ±0.016 mmol/mol in Sr/Ca_{cc} around the mean
172 could be caused by variability in Mg/Ca_{cc} (assuming Mg substitutes for Ca in the calcite lattice, and Mg
173 plus Ca approximates 1 mol per mol calcite). This may have influenced the Sr/Ca_{cc} and Na/Ca_{cc}
174 regression slopes over salinity and also the calculated inter-element correlation coefficients, but only
175 by a maximum of ±1% for both elements, which is considerably lower than the total observed
176 variability of 16% and 9%, respectively.
177

Biogeosciences Discuss., https://doi.org/10.5194/bg-2017-481
Manuscript under review for journal Biogeosciences
Discussion started: 11 December 2017

2.3 Electron Microprobe Mapping

To investigate variation of element distribution across the chamber wall, a number of cultured specimens were prepared for Electron Microprobe Analysis (EPMA). From each of the five salinity conditions, six specimens from both species were selected and embedded in resin (Araldite 2020) in an aluminum ring (diameter 1 cm) in a vacuum chamber. Samples were polished with a final polishing step using a diamond emulsion with grains of 0.04 µm. This procedure resulted in exposure of a cross-section of the foraminiferal chamber wall from which areas for EPMA mapping were selected (Appendix A). These areas were selected for being perpendicular to the shell outer surface, resulting in pores completely crossing the exposed chamber wall. Elemental distributions were mapped in chambers prior to F-3 to study the element distribution across the various layers of calcite (lamella) produced with the addition of each new chamber. Elemental distribution in the shell wall was measured using a field emission Electron Probe Micro Analyser (JEOL JXA-8530F HyperProbe) at 7.0kV with a dwell time of 350 ms, using a spot diameter of 80 nm and a step size between 0.1538 µm and 0.4072 µm (130 x 130 pixels).

Spatial resolution of the EPMA mapping was determined using the software package CASINO (monte CArlo SImulation of electroN trajectory in SOlids, v 2.48). With the input parameters identical as used in our analysis (80 nm spot size, beam current 7 KeV, etc.), the simulated surface radius of the backscattered electrons (i.e. the spatial resolution) equals 590 nm. Semi-quantitative El/Ca_{cc} profiles were calculated by averaging the El/Ca_{cc} intensities parallel to the banding direction and applying a constant calibration factor obtained from LA-ICP-MS measurements on the same specimen, similar to the procedure of Eggins et al. (2004). We did not use the depth-resolved laser ablation-profiles for this purpose, but used the average value from the profiles for correlation to the EPMA-derived intensities.

3. Results

3.1 Foraminiferal calcite element ratios and partitioning coefficients as a function of salinity

Per treatment, from lowest to highest salinity, average Na/Ca_{cc} of the newly formed calcite varied between 9.3-10.8 mmol/mol for *A. lessonii* and 4.7-6.4 mmol/mol (highest salinity) for *A. tepida* (Fig. 1), with a corresponding partition coefficient (note that partition coefficients are 'apparent', not taking into account speciation/activity of Na) ranging from $1.90*10^{-4}$ to $2.20*10^{-4}$ and from $0.97*10^{-4}$ to $1.30*10^{-4}$ for *Amphistegina* and *Ammonia*, respectively (Table 3). For both species, sets of single-specimen Na/Ca_{cc} show slightly skewed distributions towards higher Na/Ca_{cc} for all salinities (Kolmogorov- Smirnov test, at the 95% confidence level). Combining all specimens (based on the average of single-spot measurements per specimen), Na/Ca_{cc} shows a positive linear relationship with salinity for both *A. lessonii* and *A. tepida* (Na/Ca_{cc} = 0.077 ± 0.017 * S + 7.13 ± 0.60, $F_{1,186}$ = 20.9, p < 0.001 for *A. lessonii* and Na/Ca_{cc} = 0.064 ± 0.013 * S + 3.29 ± 0.44, $F_{1, 172}$ = 25.9, p < 0.001 for *A. tepida*, Fig. 1). The observed average relative standard deviation between specimens in Na/Ca_{cc} at each of the 5 salinities is 15% for *A. lessonii* and 20% for *A. tepida*. The variance in Na/Ca_{cc} between individual specimens explained by salinity is η^2=0.08 for *A. lessonii* and η^2=0.14 for *A. tepida*.

Biogeosciences Discuss., https://doi.org/10.5194/bg-2017-481
Manuscript under review for journal Biogeosciences
Discussion started: 11 December 2017

Specimen's average Mg/Ca_{cc} and Sr/Ca_{cc} correlate positively with salinity in *A. tepida* (Mg/Ca_{cc} = 0.060 ± 0.011 * S + 0.51 ± 0.38 $F_{1, 172}$ = 29.9 $p < 0.001$ and Sr/Ca_{cc} = 0.014 ± 12 * 10^{-4} * S + 1.00 ± 0.04, $F_{1, 337}$ = 254, $p < 0.001$), whereas they do not correlate with salinity in *A. lessonii*. Average relative standard deviations for the 5 salinity conditions per element are 27% for Mg/Ca_{cc} and 9% for Sr/Ca_{cc} in *A. lessonii* and 32% in Mg/Ca_{cc} and 7% for Sr/Ca_{cc} for *A. tepida*. In *A. lessonii*, the proportion of variance in Sr/Ca_{cc} explained by salinity is η^2=0.04 ($p<0.01$) (Mg/Ca_{cc} not significant) and for *A. tepida*, the proportion of variance in Sr/Ca_{cc} explained by salinity is η^2=0.44 and in Mg/Ca_{cc} η^2=0.19 ($p<0.001$).

Single-spot analyses on *Ammonia tepida* show that Na/Ca_{cc} and Mg/Ca_{cc} are significantly correlated within the salinity treatments, except for condition S=30 (Fig. 3). For the individual salinity treatments, single-spot Sr/Ca_{cc} and Mg/Ca_{cc}, as well as Na/Ca_{cc} and Sr/Ca_{cc} are not correlated significantly with each other, except for S=25. Between salinity treatments, distributions in this species shift towards higher Na/Ca_{cc}, Sr/Ca_{cc} and Mg/Ca_{cc} values with increasing salinity, although for the range between 30-40 Na/Ca_{cc} distributions remain rather similar (Fig. 3). For *Amphistegina lessonii*, distributions of Sr/Ca_{cc} and Mg/Ca_{cc} ratios overlap largely between salinities, and only Na/Ca_{cc} distributions shift towards higher values (Fig. 3). Within each salinity condition however, single-spot Na/Ca_{cc}, Mg/Ca_{cc} and Sr/Ca_{cc} in this species are positively correlated amongst each other, whereby the Na/Ca_{cc} intercept of these relationships increases with increasing salinity (Fig. 3 and Appendix C).

Table 3. Average El/Ca_{cc} ratios of the foraminiferal calcite ±standard error and corresponding apparent partitioning coefficients, defined as $D_{El}=\frac{El/Ca_{calcite}}{El/Ca_{SW}}$.

Sal	n	Na/Ca_{cc} mmol/mol	D_{Na}	Mg/Ca_{cc} mmol/mol	D_{Mg}	Sr/Ca_{cc} mmol/mol	D_{Sr}
A.l.							
S25	65	9.29±0.27	$1.90*10^{-4}$	33.35±1.20	$5.94*10^{-3}$	1.80±0.026	0.199
S30	74	9.47±0.21	$1.90*10^{-4}$	32.10±1.20	$5.64*10^{-3}$	1.74±0.020	0.189
S35	103	9.63±0.18	$1.98*10^{-4}$	32.71±1.07	$5.94*10^{-3}$	1.76±0.018	0.191
S40	50	10.25±0.31	$2.11*10^{-4}$	35.22±2.60	$6.27*10^{-3}$	1.74±0.034	0.184
S45	44	10.78±0.30	$2.20*10^{-4}$	33.80±1.68	$5.90*10^{-3}$	1.82±0.036	0.189
A.t.							
S25	109	4.75±0.11	$0.97*10^{-4}$	1.90±0.06	$3.40*10^{-4}$	1.34±0.016	0.148
S30	58	5.63±0.22	$1.13*10^{-4}$	2.41±0.09	$4.24*10^{-4}$	1.44±0.013	0.156
S35	59	5.58±0.19	$1.15*10^{-4}$	2.85±0.24	$5.17*10^{-4}$	1.50±0.012	0.163
S40	93	5.70±0.16	$1.17*10^{-4}$	2.73±0.15	$4.86*10^{-4}$	1.55±0.017	0.164
S45	20	6.39±0.37	$1.31*10^{-4}$	3.27±0.27	$5.70*10^{-4}$	1.61±0.038	0.168

3.2 Size and chamber effect on Na/Ca_{cc} and inter-specimen variance

Specimens of *A. lessonii* produced most new chambers at salinities of 25, 30 and 35, closest to the salinity in their "natural" habitat (Burgers Zoo aquarium, salinity (33.9-34.3; Ernst et al., 2011). Size averages are not significantly different between these salinity treatments, based on a Kruskal-Wallis test, whereas specimens grown at salinities 40 and 45 were significantly smaller than those from lower salinities, reflecting lower chamber addition rates over the course of the culturing experiment at higher

243 salinity (Fig. 2). Combining al specimens, Na/Ca_{cc} is not significantly related to size in *A. lessonii.*
244 Specimens of *A. tepida* produced less chambers at salinity 45, possibly because although this species is
245 used to relatively large salinity shifts in their tidal flat habitat, such a high salinity is probably close to
246 its tolerance. The lower salinity groups (25, 30, 35) produced larger specimens than the highest
247 salinities (Fig. 2). Combining al specimens, Na/Ca_{cc} is significantly related to size in *A. tepida*, yet with
248 a small slope (-0.003) and just within the 95% confidence interval (p=0.04).
249 Within each salinity tested, single-chambered Na/Ca_{cc} is slightly positively related to size for the
250 specimens of *A. lessonii* cultured at salinities 25 (slope = 0.008, $p < 0.01$), 30 (slope=0.002, $P<0.05$ and
251 35 (slope=0.005, $p<0.001$). For the same species, Mg/Ca_{cc} is positively correlated to size at salinities
252 25, 30 and 35, with a similar slope of 0.03 ($p < 0.05$). Sr/Ca_{cc} also shows a positive relationship to size
253 within salinities 25, 30 and 35 with slopes of 0.0007, 0.0003, 0.0005 ($p<0.001$) respectively. For *A.*
254 *tepida*, there is only a slight negative correlation between size and Sr/Ca_{cc} for specimens cultured at
255 salinity 25 (slope=9.9*10-4, $p<0.001$) and no significant correlation for the other conditions, or
256 between size and Na/Ca_{cc} and Mg/Ca_{cc} in all salinity groups.
257 At the lowest salinity, Na/Ca_{cc} in the F-chamber (newest chamber) show slight (0.9 mmol/mol Na/Ca
258 higher median) but significant higher values than the F-2 chambers for *A. lessonii* (multicompare test
259 based on Kruskal-Wallis test, $p<0.05$). For specimens of *A. lessonii* cultured at other salinities and for
260 *A. tepida* at any of the salinities tested, there no significant correlations between Na/Ca_{cc} and chamber
261 position were observed (note that only chamber positions F to F-2 were taken into account, as for the
262 lower chamber position sample numbers were insufficient). Furthermore, chamber position shows no
263 significant effect on Mg/Ca_{cc} and Sr/Ca_{cc}.
264 To further investigate the variance between and within individuals, a multiway ANOVA was
265 performed to investigate the effect on Na/Ca_{cc} per salinity condition. Inter-individual variance is
266 significant and larger than the variance between chamber groups and intra-individual variance in all
267 salinity groups, with the between individual variability accounting for η^2= 0.75 ± 0.11/0.84±0.03 of the
268 variance ($p<0.001$) for *A. lessonii* and *A. tepida* respectively. The variance due to chamber position is
269 not significant, and the remaining intra-individual variance accounts for η^2 = 0.09±0.05/0.08±0.05 for
270 *A. lessonii* and *A. tepida* respectively.

271 **3.3 Elemental distributions in the chamber wall**

272 EPMA maps of cross-sectioned chamber walls of *A. lessonii* show, within the resolution limits of the
273 technique, that bands of elevated Na/Ca_{cc} intensities overlap with zones of elevated Mg/Ca_{cc} (Fig. 6 and
274 appendix D). Mg bands show a higher amplitude than Na bands, but clearly coincide spatially.
275 Comparing EPMA maps with the backscatter SEM image of the exposed sections shows that the bands
276 with the highest Na/Ca_{cc} and Mg/Ca_{cc} occur in the proximity of the primary organic sheet (Fig. 4), with
277 a number of high Na- and Mg-rich bands with slightly lower maximum intensities occurring towards
278 the outer chamber surface coinciding with subsequent organic linings. For *A.tepida*, one band of
279 elevated Mg/Ca_{cc} band is visible coinciding with the POS with no clear Na/Ca_{cc} banding being
280 detected.

Biogeosciences Discuss., https://doi.org/10.5194/bg-2017-481
Manuscript under review for journal Biogeosciences
Discussion started: 11 December 2017

4. Discussion

4.1 The effect of salinity and DIC on Na/Ca_{cc}, Mg/Ca_{cc} and Sr/Ca_{cc}

The Na/Ca_{cc} single-specimen data of the cultured *A. lessonii* and *A. tepida* both correlate positively with salinity (Table 3, Fig. 1). This is in line with previous calibrations (for *Ammonia tepida*; Wit et al., 2013, for cultured *Globigerinoides ruber*; (Allen et al., 2016) and for field-collected *G. ruber* and *G. sacculifer*; Mezger et al. (2016)). However, our Na/Ca-salinity calibration for *A. tepida* is somewhat less sensitive than that observed earlier for the same species (Wit et al., 2013). An offset in Na/Ca_{cc} values between calibrations for a single species has been reported before (e.g. Mezger et al., 2016 and Allen et al., 2016 for the planktonic *G. ruber* and *G. sacculifer*). Such an apparent discrepancy between studies may be caused by differences in one of the not targeted conditions between cultures or in situ conditions (e.g. carbon chemistry, light intensity). Alternatively, subtle analytical differences (e.g. differences in cleaning procedures), statistical reasons (for example differences in the number of analyses or sample size) or the effect of genotypic variability on element incorporation (Sadekov et al., 2016) may also play a role. Although the calibration presented here consists of much more data points compared to those in Wit et al. (2013), we do not want to dismiss the latter as several parameters (like cleaning procedures) inevitably might not have been identical. As such the difference observed between studies merely illustrates the potential range for this species.

Contrasts in sensitivities such as observed for Na/Ca_{cc} between calibrations also apply to Mg/Ca_{cc} and Sr/Ca_{cc}, both of which here show an increase with salinity in *A. tepida* but not in *A. lessonii* (Fig. 1). Previous culturing experiments with *Ammonia tepida*, however, showed a smaller sensitivity of Mg/Ca_{cc} to salinity (0.029-0.0044 mmol/mol change per salinity unit; Dissard et al., 2010) than that reported here (0.06). Still, all these sensitivities are considerably lower than that reported in Kisakürek et al. (2008) for the planktonic *G. ruber* (0.23 when Mg/Ca_{cc} is assumed to increase linearly with salinity), but in the same range as that reported by Nürnberg et al. (1996) for *G. sacculifer* (0.05). The sensitivity of Sr/Ca_{cc} to salinity in *A. tepida* (0.014; Table 3) is comparable to that for *O. universa* (0.008; Lea et al., 2008), *G. ruber* (0.02; Kisakürek et al., 2008) and similar to the significant effect of salinity on Sr incorporation in the same species (0.01-0.02, depending on temperature) found by Dissard et al. (2010).

Seawater carbonate chemistry is an additional factor potentially affecting trace metal uptake (e.g. Lea et al., 1999; Keul et al., 2017; Russell et al., 2004). Since salinity and dissolved inorganic carbon concentration in the culture media co-varied in our experiments similar to the natural environment (Table 1), Na/Ca_{cc} in our cultured specimens also correlates positively to seawater [DIC]. However, sodium incorporation has been shown to be independent from changes in carbonate chemistry in cultured *Amphistegina gibbosa* and several other benthic hyaline and porcelaneous species (Van Dijk et al., 2017a). Additionally, Allen et al., (2016) also found no significant effect of carbonate chemistry (i.e. varying $[CO_3^{2-}]$) on Na incorporation in cultured *G. ruber*, suggesting that the variability in Na/Ca_{cc} observed here in *A. lessonii* can be attributed to changes in salinity rather than [DIC]. Previous studies showed that Sr/Ca_{cc} correlates positively to [DIC] in *A. tepida* (Keul et al., 2017), which may account for part of the correlation between Sr/Ca_{cc} and salinity reported here for this species. The

published sensitivity of Sr/Ca_{cc} to [DIC] is approximately $2*10^{-5}$ mmol/mol change in Sr/Ca_{cc} for every 1 µmol/kg change in [DIC], likely representing the maximum potential effect of DIC on Sr partitioning given that others found no significant effect (Dissard et al., 2010a). For a change in ~850 µmol/kg (Table 1), this would amount to an increase in Sr/Ca_{cc} of 0.019 mmol/mol (Keul et al., 2017) over the salinity range studied here, thereby accounting for approximately 7% of the total observed change in Sr/Ca_{cc} (Table 3). Inorganic carbon chemistry is known to affect growth rates and shell weights in benthic foraminifera (Dissard et al., 2010a; Keul et al., 2013), which in turn, may affect incorporation of Sr and Mg, hence providing a mechanistic link between inorganic carbon chemistry and element partitioning.

The absence of an (strong) impact of DIC on Mg/Ca_{cc} in foraminiferal calcite (our results; Fig. 1; Kısakürek et al., 2008; Dissard et al., 2010a; Russell et al., 2004) implies that changes in combined Mg/Ca_{cc} and Na/Ca_{cc} in low-Mg foraminiferal species can be used to reconstruct salinity and improve temperature estimates. Any additional changes in the marine inorganic carbon system will have a much larger impact on other elements (e.g. B, Zn, U), so that the combined analyses of all these elements will allow for a complete reconstruction of past seawater conditions.

El/Ca ratios of specimens of both species grown within each salinity condition are characterized by a relatively large variability. Of the overall data set salinity only explains around 8% of the variation in Na incorporation for *A. lessonii* and 14% 19% and 44% of Na, Mg and Sr incorporation. However, for *A. lessonii*, the mean values (which translates to the values obtained from traditional solution-ICP-MS) fit the regression model relatively well (Fig. 1). However, given the low sensitivity, many specimens are required to reduce the uncertainty (Appendix E). This is reflected by the relatively wide prediction bounds for the Na/Ca-salinity regressions, indicating an uncertainty associated with a single Na/Ca_{cc} measurement. The relatively inter-specimen variability in element/Ca_{cc} ratios has been reported and discussed before (e.g. Sadekov et al., 2008; De Nooijer et al., 2014a), but the cause for this variability remains to be identified.

4.2 El/Ca_{cc} variability at the inter-specimen and inter-species level

Single-chamber measurements show that Na/Ca_{cc} for both species varies between chambers (i.e. specimens) with a RSD of 15%-20%, despite identical culture conditions (Fig. 1). Since the analytical error on Na/Ca_{cc} accounts for approximately 2% (Table 2), a large portion of the observed variability between specimens must be due to ontogeny and/or inter-specimen differences in biomineralization controls (De Nooijer et al., 2014).

Foraminiferal shell size at salinities 40 and 45 are significantly smaller than those cultured at lower salinities. When combining data from all salinities, however, there is no (*A. lessonii*) or only a very small (*A. tepida*) negative correlation between Na/Ca_{cc} and shell size, as suggested earlier by Wit et al. (2013). Potentially the earlier observed co-variation was caused by an indirect co-variation rather than a causal relationship. Also within treatments, a relationship between Na/Ca_{cc} and size is either opposite (i.e. positive) or absent. Hence, size is unlikely to be responsible for any of the observed inter-specimen variability in $Na/Ca_{cc,}$ which is supported by the absence of a correlation between chamber position (and hence ontogenetic stage) and Na/Ca_{cc}. This implies that differences in Na/Ca_{cc} between chambers

359 do not need to be taken into account when applying Na/Ca_{cc} as a proxy, although the large inter-
360 specimen variance in Na/Ca_{cc} requires sufficient specimens (n>30, for an error margin <5% at the 95%
361 confidence level; Sadekov et al., 2008; De Nooijer et al., 2014a) to be analyzed. As most variability is
362 between individuals rather than between chambers (section 3.3), analyzing more chambers of the same
363 specimen does not necessarily improve the precision of the salinity estimate. Without a major effect of
364 ontogeny, physiological processes at the organismal level are more likely to cause observed large inter-
365 specimen variability in Na/Ca_{cc}.
366 In *A. lessonii*, single-spot Na/Ca_{cc}, Sr/Ca_{cc} and Mg/Ca_{cc} are correlated amongst each other within each
367 salinity condition (Fig. 3). Correlation coefficients between the three element ratios are similar for the
368 different salinities, with superimposed an increase in the Na/Ca_{cc} relative to that of Mg/Ca_{cc} and Sr/Ca_{cc}
369 with increasing salinity (Appendix C). In contrast, single-spot Sr/Ca_{cc} and Mg/Ca_{cc} in *A. tepida* are not
370 correlated, whereas incorporation of all these elements increases significantly with salinity. Within
371 salinities Mg/Ca_{cc} and Na/Ca_{cc} are significantly correlated in 4 out of the 5 salinities, but with much
372 lower correlation coefficients compared to *A. lessonii* (Fig. 3 and Appendix C). However, between the
373 different salinities these elements are correlated in *A. tepida*, implying that for *A. tepida* salinity is one
374 of the actual parameters controlling element uptake.
375 The differences in (an absence of) a correlation between elements between the two species
376 studied here likely reflect differences in their calcification pathways. At the same time, such a
377 difference may also explain why Sr/Ca_{cc} and Mg/Ca_{cc} are correlated to salinity in *A. tepida*, but not in
378 *A. lessonii* (4.1). The overall element composition of the calcite precipitated by *A. lessonii* suggests that
379 the calcification process of this species may more closely resemble inorganic calcite precipitation,
380 compared to *Ammonia tepida* and other low-Mg calcite precipitating species. In the intermediate-Mg
381 calcite species, crystal lattice strain is elevated which may promote incorporation of other elements
382 through stress compensation (Mucci and Morse, 1983; Mewes et al., 2015). This would explain the
383 observed inter-element correlations within salinities. Another difference between the species studied
384 here may be caused by differences in $CaCO_3$ phase shifts during calcite precipitation (e.g. Bots et al.,
385 2012; De Yoreo et al., 2015). A metastable vaterite pre-cursor phase recently found in two planktonic
386 species may explain the low Mg incorporation relative to inorganic calcite (Jacob et al., 2017). The
387 higher Mg contents of *A. lessonii* could be related to the (partial) absence of a vaterite-calcite
388 transformation in this species. A higher Mg concentration at the site of calcification might result in a
389 phase shift from amorphous calcium carbonate (ACC) directly into to calcite, with Mg stabilising the
390 ACC, as described by Littlewood et al. (2017). The absence of a vaterite precursor phases also
391 enhances the incorporation of other metals incompatible to calcite, such as Sr (Littlewood et al, 2017)
392 and hence may contribute to the inter-species differences in element partitioning similar to that
393 observed here. Although the strong fractionation against Mg in *A. tepida* could reflect double
394 fractionation through a vaterite-calcite transformation (Jacob et al., 2017) the low-Mg content might as
395 well reflect a more enclosed site of calcification, whereby ions are mainly transported trans-membrane
396 (Nehrke et al., 2013), but the experiments here do not allow distinguishing these two potential
397 mechanisms. Trans-membrane transport (TMT) of Ca^{2+} and concomitant leakage of Mg^{2+} and Sr^{2+}
398 might be more sensitive to differences in ionic strength and element concentrations, hence possibly

399 explaining the salinity effect on the incorporation of these elements in *A. tepida* whereas it does not in
400 *A. lessonii*, assuming that TMT relatively contributes more to the supply of ions to the site of
401 calcification in this species compared to *A. lessonii*, which might be relatively more dependent on
402 seawater vacuolisation.

403 **4.3 Intra-specimen variability**

404 In both species, Mg is found to be elevated in bands located close to the primary organic sheet and
405 (often less pronounced) to other organic layers (Fig. 4), present in rotaliid species due to their lamellar
406 calcification mode (Reiss, 1957, 1960). This is similar to reports of within-chamber wall banding in
407 many elements in other species (Branson et al., 2016; Eggins et al., 2004; Sadekov et al., 2005; Paris et
408 al., 2014; Spero et al., 2015; Fehrenbacher et al., 2017; Kunioka et al., 2006; Steinhardt et al., 2015;
409 Hathorne et al., 2009). As in other studies, the Na- and Mg- bands are spatially correlated (Fig. 4). For
410 *Ammonia tepida*, the banding in both elements is less pronounced than for *Amphistegina lessonii*,
411 which is not surprising given the higher average El/Ca_{cc} ratios in the latter species. This inter-species
412 difference observed in the Mg- and Na-maps implies that the concentration of Mg and Na within the
413 high concentration band is lower in *A. tepida* than in *A. lessonii*. Alternatively, as the observations are
414 close to the spatial resolution of the method, the observed pattern could also be due to the band's width
415 being smaller in *A. tepida* compared to *A. lessonii*. When comparing the distribution of the two
416 elements within one specimen, the Mg/Ca_{cc} bands are more pronounced than those of Na/Ca_{cc},
417 particularly for *A. lessonii* (Fig. 4).
418 The spatial correlation between the intra-shell distributions Mg and Na suggests a coupled control on
419 these elements during the calcification process, which is in line with the observed inter-specimen
420 correlations. This suggests that the incorporation of these cations is influenced by similar
421 biomineralization mechanisms, related to seawater vacuolization (Erez, 2003; Bentov and Erez, 2006),
422 trans-membrane transport of elements (Nehrke et al., 2013) and/or metastable precursor phases (Jacob
423 et al., 2017). The relative contributions of these mechanisms might differ between species, resulting in
424 the observed differences in element incorporation between species. Differences in the efficiency of
425 such processes between specimens might cause the observed inter-specimen variability, whereas
426 changes in these processes during the calcification time could be responsible for the observed
427 correlation between elements within the chamber wall.

428 **5. Conclusions**

429 By extending existing calibrations of the Na/Ca_{cc}-salinity proxy to the intermediate-Mg calcite
430 precipitating benthic foraminifer *Amphistegina lessonii*, we show that the Na/Ca_{cc} increase as a
431 function of salinity is similar to that in previously studied species. The absolute Na/Ca_{cc} for *A. lessonii*
432 is, however, higher than that in *Ammonia tepida*. In *A. tepida*, Mg/Ca_{cc} and Sr/Ca_{cc} are positively
433 correlated to salinity, whereas they are not impacted by salinity in *A. lessonii*. Within each salinity,
434 single chamber-Na/Ca_{cc} and Mg/Ca_{cc} are positively correlated in *A. tepida*, whereas single chamber-
435 Sr/Ca_{cc} is not correlated to either Mg/Ca_{cc} or Na in this species. For *A. lessonii*, all Sr/Ca_{cc}, Mg/Ca_{cc} and

436 Na/Ca_{cc} combinations are positively correlated at the single chamber level. EPMA mapping of Na and
437 Mg within chamber walls of cultured specimens shows that in *A. lessonii*, Na/Ca_{cc} and Mg/Ca_{cc} occur
438 in elevated bands in close proximity to the primary organic lining. For specimens of *A. tepida*, Mg-
439 banding appears similar to that in *A. lessonii*, whereas Na-banding is less prominent in this species.

440 **Acknowledgements**

441 We would like to thank Wim Boer for assistance with LA-ICP-MS measurements, Patrick Laan for
442 seawater measurements and Karel Bakker for DIC measurements. We kindly thank Max Janse
443 (Burgers Zoo, Arnhem) for providing stock specimens of *A. lessonii* and Kirsten Kooijmans (NIOZ)
444 for providing cultures of *Dunaliella salina*. Sergei Matveev is thanked for assistance with the Electron
445 Microprobe analysis and Leonard Bik for assistance with polishing the samples. This work was carried
446 out under the program of the Netherlands Earth System Science Centre (NESSC), financially supported
447 by the Ministry of Education, Culture and Science (OCW) (Grantnr. 024.002.001) and Darwin Centre
448 for Biogeosciences (program 3020).

449 **References**

450 Allen, K. A., Hönisch, B., Eggins, S. M., Haynes, L. L., Rosenthal, Y., and Yu, J.: Trace element
451 proxies for surface ocean conditions: A synthesis of culture calibrations with planktic foraminifera,
452 Geochimica et Cosmochimica Acta, 193, 197-221, 2016.
453 Anand, P., Elderfield, H., and Conte, M. H.: Calibration of Mg/Ca thermometry in planktonic
454 foraminifera from a sediment trap time series, Paleoceanography, 18, 10.1029/2002kpa000846, 2003.
455 Bemis, B. E., Spero, H. J., Bijma, J., and Lea, D. W.: Reevaluation of the oxygen isotopic composition
456 of planktonic foraminifera: Experimental results and revised paleotemperature equations,
457 Paleoceanography, 13, 150-160, 10.1029/98pa00070, 1998.
458 Bentov, S., and Erez, J.: Impact of biomineralization processes on the Mg content of foraminiferal
459 shells: A biological perspective, Geochemistry Geophysics Geosystems, 7, 10.1029/2005gc001015,
460 2006.
461 Bots, P., Benning, L. G., Rodriguez-Blanco, J.-D., Roncal-Herrero, T., and Shaw, S.: Mechanistic
462 insights into the crystallization of amorphous calcium carbonate (ACC), Crystal Growth & Design, 12,
463 3806-3814, 2012.
464 Branson, O., Bonnin, E. A., Perea, D. E., Spero, H. J., Zhu, Z., Winters, M., Hönisch, B., Russell, A.
465 D., Fehrenbacher, J. S., and Gagnon, A. C.: Nanometer-Scale Chemistry of a Calcite Biomineralization
466 Template: Implications for Skeletal Composition and Nucleation, Proceedings of the National
467 Academy of Sciences, 201522864, 2016.
468 De Nooijer, L. J., Hathorne, E. C., Reichart, G. J., Langer, G., and Bijma, J.: Variability in calcitic
469 Mg/Ca and Sr/Ca ratios in clones of the benthic foraminifer *Ammonia tepida*, Marine
470 Micropaleontology, 107, 32-43, 10.1016/j.marmicro.2014.02.002, 2014.
471 De Nooijer, L. J., Brombacher, A., Mewes, A., Langer, G., Nehrke, G., Bijma, J., and Reichart, G.-J.:
472 Ba incorporation in benthic foraminifera, Biogeosciences Discuss., 1-35, 2017.
473 De Yoreo, J. J., Gilbert, P. U., Sommerdijk, N. A., Penn, R. L., Whitelam, S., Joester, D., Zhang, H.,
474 Rimer, J. D., Navrotsky, A., and Banfield, J. F.: Crystallization by particle attachment in synthetic,
475 biogenic, and geologic environments, Science, 349, aaa6760, 2015.
476 Dissard, D., Nehrke, G., Reichart, G.-J., and Bijma, J.: Impact of seawater pCO2 on calcification and
477 Mg/Ca and Sr/Ca ratios in benthic foraminifera calcite: results from culturing experiments with
478 Ammonia tepida, Biogeosciences, 7, 81-93, 2010a.
479 Dissard, D., Nehrke, G., Reichart, G. J., and Bijma, J.: The impact of salinity on the Mg/Ca and Sr/Ca
480 ratio in the benthic foraminifera *Ammonia tepida*: Results from culture experiments, Geochimica Et
481 Cosmochimica Acta, 74, 928-940, 10.1016/j.gca.2009.10.040, 2010b.

Diz, P., Barras, C., Geslin, E., Reichart, G.-J., Metzger, E., Jorissen, F., and Bijma, J.: Incorporation of Mg and Sr and oxygen and carbon stable isotope fractionation in cultured Ammonia tepida, Marine Micropaleontology, 92, 16-28, 2012.

Duenas-Bohorquez, A., da Rocha, R. E., Kuroyanagi, A., de Nooijer, L. J., Bijma, J., and Reichart, G. J.: Interindividual variability and ontogenetic effects on Mg and Sr incorporation in the planktonic foraminifer *Globigerinoides sacculifer*, Geochimica Et Cosmochimica Acta, 75, 520-532, 10.1016/j.gca.2010.10.006, 2011.

Dueñas-Bohórquez, A., da Rocha, R. E., Kuroyanagi, A., Bijma, J., and Reichart, G.-J.: Effect of salinity and seawater calcite saturation state on Mg and Sr incorporation in cultured planktonic foraminifera, Marine Micropaleontology, 73, 178-189, 2009.

Eggins, S. M., Sadekov, A., and De Deckker, P.: Modulation and daily banding of Mg/Ca in *Orbulina universa* tests by symbiont photosynthesis and respiration: a complication for seawater thermometry?, Earth and Planetary Science Letters, 225, 411-419, 10.1016/j.epsl.2004.06.019, 2004.

Elderfield, H., and Ganssen, G.: Past temperature and delta O-18 of surface ocean waters inferred from foraminiferal Mg/Ca ratios, Nature, 405, 442-445, 10.1038/35013033, 2000.

Erez, J.: The source of ions for biomineralization in foraminifera and their implications for paleoceanographic proxies, Biomineralization, 54, 115-149, 10.2113/0540115, 2003.

Ernst, S., Janse, M., Renema, W., Kouwenhoven, T., Goudeau, M. L., and Reichart, G. J.: Benthic foraminifera in a large indo-pacific coral reef aquarium, Journal of Foraminiferal Research, 41, 101-113, 2011.

Fehrenbacher, J. S., Russell, A. D., Davis, C. V., Gagnon, A. C., Spero, H. J., Cliff, J. B., Zhu, Z., and Martin, P.: Link between light-triggered Mg-banding and chamber formation in the planktic foraminifera *Neogloboquadrina dutertrei*, Pacific Northwest National Laboratory (PNNL), Richland, WA (US), Environmental Molecular Sciences Laboratory (EMSL), 2017.

Guillong, M., Meier, D. L., Allan, M. M., Heinrich, C. A., and Yardley, B. W.: Appendix A6: SILLS: A MATLAB-based program for the reduction of laser ablation ICP-MS data of homogeneous materials and inclusions, Mineralogical Association of Canada Short Course, 40, 328-333, 2008.

Hathorne, E. C., James, R. H., and Lampitt, R. S.: Environmental versus biomineralization controls on the intratest variation in the trace element composition of the planktonic foraminifera *G. inflata* and *G. scitula*, Paleoceanography, 24, 10.1029/2009pa001742, 2009.

Hönisch, B., Allen, K. A., Lea, D. W., Spero, H. J., Eggins, S. M., Arbuszewski, J., Rosenthal, Y., Russell, A. D., and Elderfield, H.: The influence of salinity on Mg/Ca in planktic foraminifers–Evidence from cultures, core-top sediments and complementary δ 18 O, Geochimica et Cosmochimica Acta, 121, 196-213, 2013.

Jacob, D., Wirth, R., Agbaje, O., Branson, O., and Eggins, S.: Planktic foraminifera form their shells via metastable carbonate phases, Nature Communications, 8, 1265, 2017.

Keul, N., Langer, G., de Nooijer, L. J., and Bijma, J.: Effect of ocean acidification on the benthic foraminifera Ammonia sp. is caused by a decrease in carbonate ion concentration, Biogeosciences, 10, 6185-6198, 2013.

Keul, N., Langer, G., Thoms, S., de Nooijer, L. J., Reichart, G.-J., and Bijma, J.: Exploring foraminiferal Sr/Ca as a new carbonate system proxy, Geochimica et Cosmochimica Acta, 202, 374-386, 2017.

Kısakürek, B., Eisenhauer, A., Böhm, F., Garbe-Schönberg, D., and Erez, J.: Controls on shell Mg/Ca and Sr/Ca in cultured planktonic foraminiferan, Globigerinoides ruber (white), Earth and Planetary Science Letters, 273, 260-269, 2008.

Kunioka, D., Shirai, K., Takahata, N., Sano, Y., Toyofuku, T., and Ujiie, Y.: Microdistribution of Mg/Ca, Sr/Ca, and Ba/Ca ratios in *Pulleniatina obliquiloculata* test by using a NanoSIMS: Implication for the vital effect mechanism, Geochemistry Geophysics Geosystems, 7, 10.1029/2006gc001280, 2006.

Lea, D. W., Mashiotta, T. A., and Spero, H. J.: Controls on magnesium and strontium uptake in planktonic foraminifera determined by live culturing, Geochimica Et Cosmochimica Acta, 63, 2369-2379, 10.1016/s0016-7037(99)00197-0, 1999.

Littlewood, J. L., Shaw, S., Peacock, C. L., Bots, P., Trivedi, D., and Burke, I. T.: Mechanism of Enhanced Strontium Uptake into Calcite via an Amorphous Calcium Carbonate Crystallization Pathway, Crystal Growth & Design, 17, 1214-1223, 2017.

Mewes, A., Langer, G., de Nooijer, L. J., Bijma, J., and Reichart, G. J.: Effect of different seawater Mg2+ concentrations on calcification in two benthic foraminifers, Marine Micropaleontology, 113, 56-64, 10.1016/j.marmicro.2014.09.003, 2014.

Mewes, A., Langer, G., Reichart, G.-J., de Nooijer, L. J., Nehrke, G., and Bijma, J.: The impact of Mg contents on Sr partitioning in benthic foraminifers, Chemical Geology, 412, 92-98, 2015.

Mezger, E., Nooijer, L., Boer, W., Brummer, G., and Reichart, G.: Salinity controls on Na incorporation in Red Sea planktonic foraminifera, Paleoceanography, 2016.
Mucci, A., and Morse, J. W.: The incorporation of Mg2+ and Sr2+ into calcite overgrowths: influences of growth rate and solution composition, Geochimica et Cosmochimica Acta, 47, 217-233, http://dx.doi.org/10.1016/0016-7037(83)90135-7, 1983.
Nehrke, G., Keul, N., Langer, G., de Nooijer, L. J., Bijma, J., and Meibom, A.: A new model for biomineralization and trace-element signatures of Foraminifera tests, Biogeosciences, 10, 6759-6767, 10.5194/bg-10-6759-2013, 2013.
Nürnberg, D., Bijma, J., and Hemleben, C.: Assessing the reliability of magnesium in foraminiferal calcite as a proxy for water mass temperatures, Geochimica et Cosmochimica Acta, 60, 803-814, 1996.
Paris, G., Fehrenbacher, J. S., Sessions, A. L., Spero, H. J., and Adkins, J. F.: Experimental determination of carbonate-associated sulfate delta S-34 in planktonic foraminifera shells, Geochemistry Geophysics Geosystems, 15, 1452-1461, 10.1002/2014gc005295, 2014.
Raja, R., Saraswati, P. K., and Iwao, K.: A field□based study on variation in Mg/Ca and Sr/Ca in larger benthic foraminifera, Geochemistry, Geophysics, Geosystems, 8, 2007.
Reichart, G. J., Jorissen, F., Anschutz, P., and Mason, P. R. D.: Single foraminiferal test chemistry records the marine environment, Geology, 31, 355-358, 10.1130/0091-7613(2003)031<0355:sftcrt>2.0.co;2, 2003.
Reiss, Z.: The Bilamellidea, nov. superfam., and remarks on Cretaceous globorotaliids, Contrib Cushman Found Foram Res, 8, 127-145, 1957.
Reiss, Z.: Structure of so-called Eponides and some other rotaliiform foraminifera, State of Israel, Ministry of Development, Geological Survey, 1960.
Rosenthal, Y., Lohmann, G. P., Lohmann, K. C., and Sherrell, R. M.: Incorporation and preservation of Mg in *Globigerinoides sacculifer:* Implications for reconstructing the temperature and O-18/O-16 of seawater, Paleoceanography, 15, 135-145, 10.1029/1999pa000415, 2000.
Russell, A. D., Hönisch, B., Spero, H. J., and Lea, D. W.: Effects of seawater carbonate ion concentration and temperature on shell U, Mg, and Sr in cultured planktonic foraminifera, Geochimica et Cosmochimica Acta, 68, 4347-4361, 2004.
Sadekov, A. Y., Eggins, S. M., and De Deckker, P.: Characterization of Mg/Ca distributions in planktonic foraminifera species by electron microprobe mapping, Geochemistry Geophysics Geosystems, 6, 10.1029/2005gc000973, 2005.
Segev, E., and Erez, J.: Effect of Mg/Ca ratio in seawater on shell composition in shallow benthic foraminifera, Geochemistry Geophysics Geosystems, 7, 10.1029/2005gc000969, 2006.
Spero, H. J., Eggins, S. M., Russell, A. D., Vetter, L., Kilburn, M. R., and Honisch, B.: Timing and mechanism for intratest Mg/Ca variability in a living planktic foraminifer, Earth and Planetary Science Letters, 409, 32-42, 10.1016/j.epsl.2014.10.030, 2015.
Steinhardt, J., de Nooijer, L. L., Brummer, G. J., and Reichart, G. J.: Profiling planktonic foraminiferal crust formation, Geochemistry, Geophysics, Geosystems, 16, 2409-2430, 2015.
Stoll, M. H. C., Bakker, K., Nobbe, G. H., and Haese, R. R.: Continuous-flow analysis of dissolved inorganic carbon content in seawater, Analytical Chemistry, 73, 4111-4116, 10.1021/ac010303r, 2001.
Terakado, Y., Ofuka, Y., and Tada, N.: Rare earth elements, Sr, Ba, Fe, and major cation concentrations in some living foraminiferal tests collected from Iriomote Island, Japan: An exploration for trace element behavior during biogenic calcium carbonate formation, Geochemical Journal, 44, 315-322, 2010.
Toyofuku, T., Kitazato, H., Kawahata, H., Tsuchiya, M., and Nohara, M.: Evaluation of Mg/Ca thermometry in foraminifera: Comparison of experimental results and measurements in nature, Paleoceanography, 15, 456-464, 10.1029/1999pa000460, 2000.
Toyofuku, T., Suzuki, M., Suga, H., Sakai, S., Suzuki, A., Ishikawa, T., de Nooijer, L. J., Schiebel, R., Kawahata, H., and Kitazato, H.: Mg/Ca and δ 18 O in the brackish shallow-water benthic foraminifer *Ammonia 'beccarii'*, Marine Micropaleontology, 78, 113-120, 2011.
Van Dijk, I., de Nooijer, L. J., and Reichart, G.-J.: Trends in element incorporation in hyaline and porcelaneous foraminifera as a function of pCO 2, Biogeosciences, 14, 497, 2017a.
Van Dijk, I., de Nooijer, L. J., Wolthers, M., and Reichart, G.-J.: Impacts of pH and [CO 3 2−] on the incorporation of Zn in foraminiferal calcite, Geochimica et Cosmochimica Acta, 197, 263-277, 2017b.
Wit, J. C., de Nooijer, L. J., Wolthers, M., and Reichart, G. J.: A novel salinity proxy based on Na incorporation into foraminiferal calcite, Biogeosciences, 10, 6375-6387, 10.5194/bg-10-6375-2013, 2013.

Biogeosciences Discuss., https://doi.org/10.5194/bg-2017-481
Manuscript under review for journal Biogeosciences
Discussion started: 11 December 2017

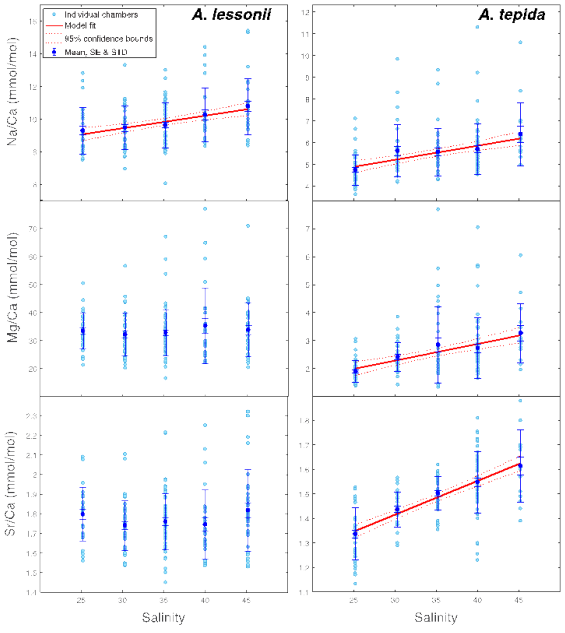

Figure 1. Foraminiferal Na/Ca_{cc}, Mg/Ca_{cc} and Sr/Ca_{cc} versus salinity. Light blue dots represent the average per specimen (n= 359 for A. lessonii, n= for A. tepida, with ±3 measured chambers per individual), dark blue dots indicate the mean, with inner error bars indicating the standard error and outer error bars the standard deviation for each treatment. The linear regression model (red line) is based on the individuals' mean, with the 95% confidence interval of the regression in dashed lines.

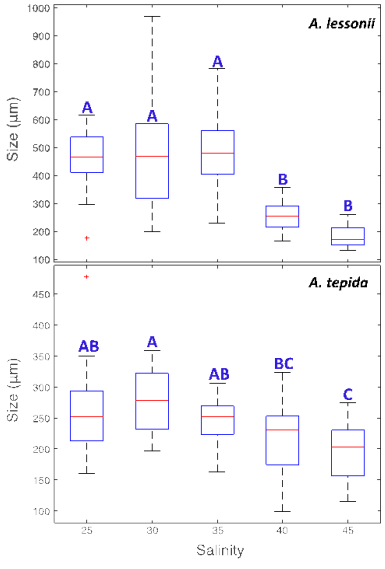

Biogeosciences Discuss., https://doi.org/10.5194/bg-2017-481
Manuscript under review for journal Biogeosciences
Discussion started: 11 December 2017

Figure 2. Boxplot showing the size distributions (median, 1st and 3rd quartiles, minimum and maximum values) for each salinity condition, n=68, 74, 115, 53, 45 for *A. lessonii* and n= ... for *A. tepida*. Letters indicate significant different population means, based on ANOVA (p<0.001).

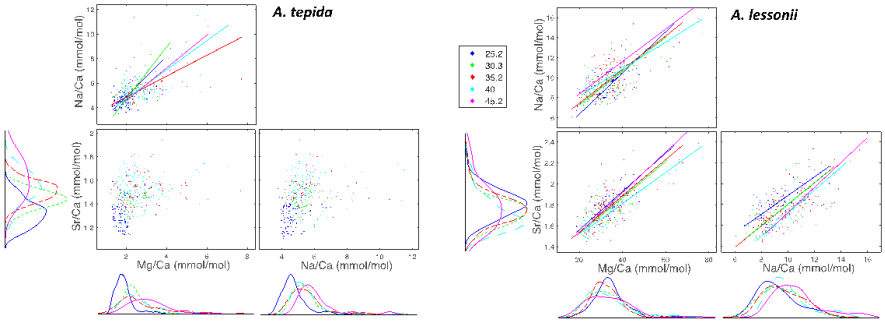

Figure 3. Individual chamber LA-ICP-MS analyses showing correlations between foraminiferal Mg/Ca_{cc}, Sr/Ca_{cc} and Na/Ca_{cc} for *A. tepida* (left) and *A. lessonii* (right) per salinity condition. Significant orthogonal linear regressions for are indicted with a line, colour coded for salinity (see legend). Correlation coefficients, slope and intercepts of these regressions can be found in Appendix C. Within salinity conditions, element ratios are strongly correlated with each other in *A. lessonii*, whereas in *A. tepida*, element ratios do not (strongly) correlate with each other. When combining all single-spot data in *A. tepida*, element ratios correlate amongst each other because the incorporation of all three elements increases with salinity, shifting the distributions to higher values. In *A. lessonii*, only the Na/Ca_{cc} distributions shift towards higher values with increasing salinity, whereas Mg/Ca_{cc} and Sr/Ca_{cc} distributions are relatively similar between salinity conditions.

Biogeosciences Discuss., https://doi.org/10.5194/bg-2017-481
Manuscript under review for journal Biogeosciences
Discussion started: 11 December 2017

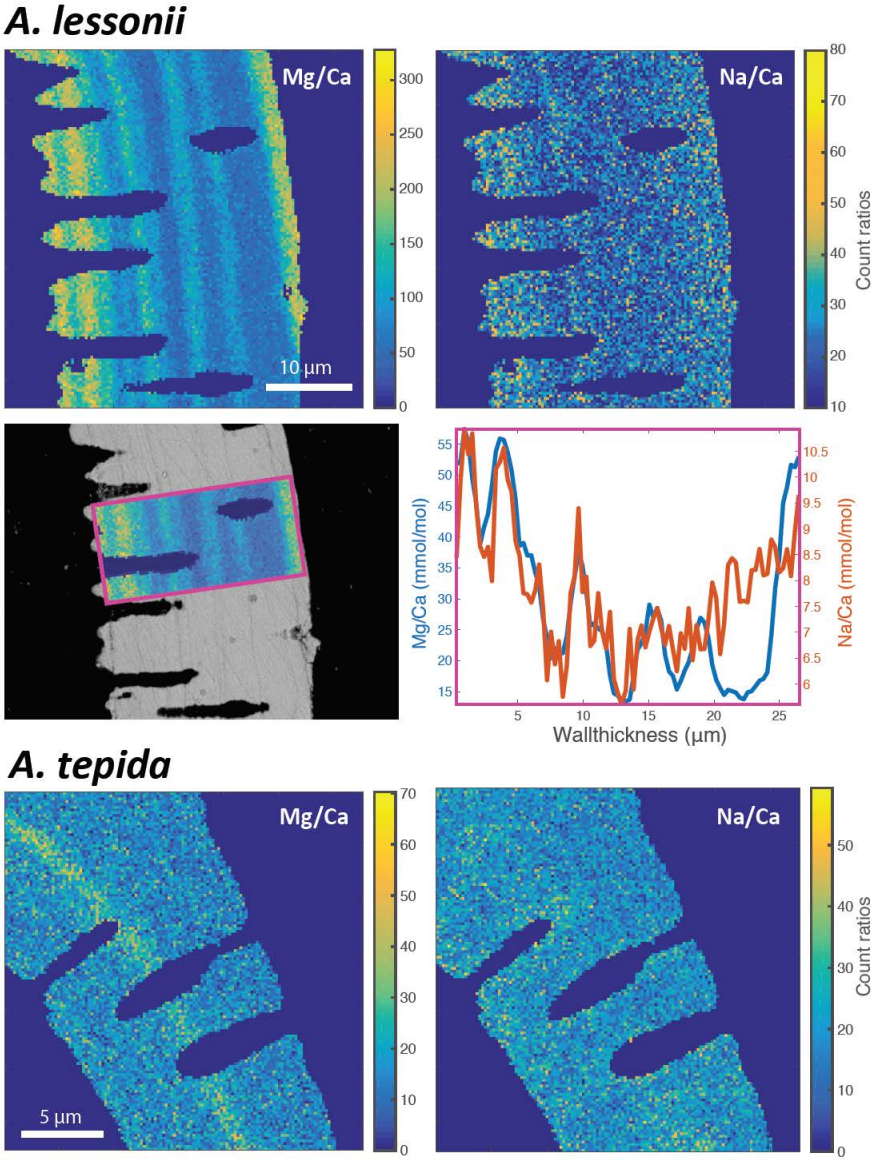

Figure 4. Foraminiferal Mg/Ca_{cc} (upper left) and Na/Ca_{cc} (upper right) intensity ratio maps, obtained with EPMA, for a specimen of *A. lessonii* grown at a salinity of 30. The lower right panel shows profiles for Mg/Ca (blue) and Na/Ca (red), based on averaged EPMA ratios scaled to LA-ICP-MS measurements of the same specimen, of an averaged transact area through the chamber wall perpendicular to the POS. The transect area is indicated in the lower left panel, on top of a backscatter SEM image, showing that the high El/Ca bands overlap with the primary organic sheet (POS, left) and subsequent organic linings (towards the right). Correlation coefficient R^2=0.56 ($p<0.001$) for Mg versus Na, based on element intensity counts to exclude covariation with Ca. Lower panels show Mg/Ca_{cc} (lower left) and Na/Ca_{cc} (lower right) intensity

ratio maps, obtained with EPMA, for a specimen of *A. tepida* grown at a salinity of 35. See C for the results for three more specimen.

Appendix

Appendix A.

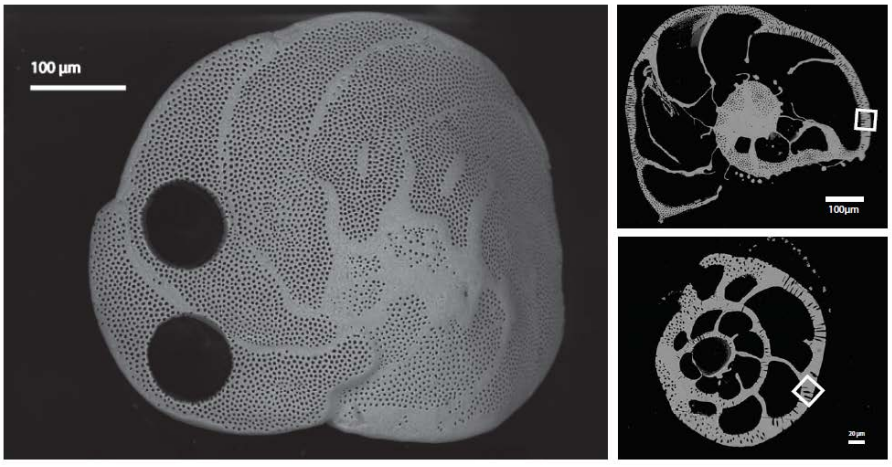

SEM image of a specimen of *A. lessonii* showing LA-ICP-MS measurement spots (left) and SEM images of specimens of *A. lessonii* (upper right) and *A. tepida* (lower right) embedded in resin and polished for Electron Probe Micro Analysis, the mapping area is depicted with a white box.

Appendix B.

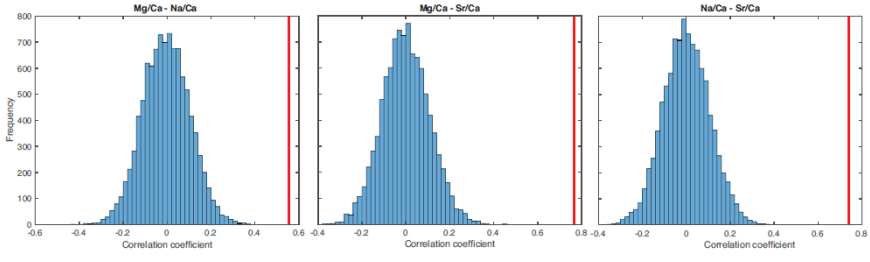

Results of the Monte Carlo analysis showing that the measured correlation coefficients for the inter-specimen correlations between the measured El^1/Ca_{cc} and El^2/Ca_{cc} are not caused by a spurious correlation due to the common denominator Ca_{cc}, showing that the measured correlation coefficient is significantly higher then the distribution of the correlation coefficients between 10.000 randomly drawn El^1 concentrations/measured Ca concentration and measured El^2/Ca concentrations. This test is based on the concentration results from a single labbook (measurement run) with specimens of *A. lessonii* cultured at a salinity of 35.

Biogeosciences Discuss., https://doi.org/10.5194/bg-2017-481
Manuscript under review for journal Biogeosciences
Discussion started: 11 December 2017

649 **Appendix C.**

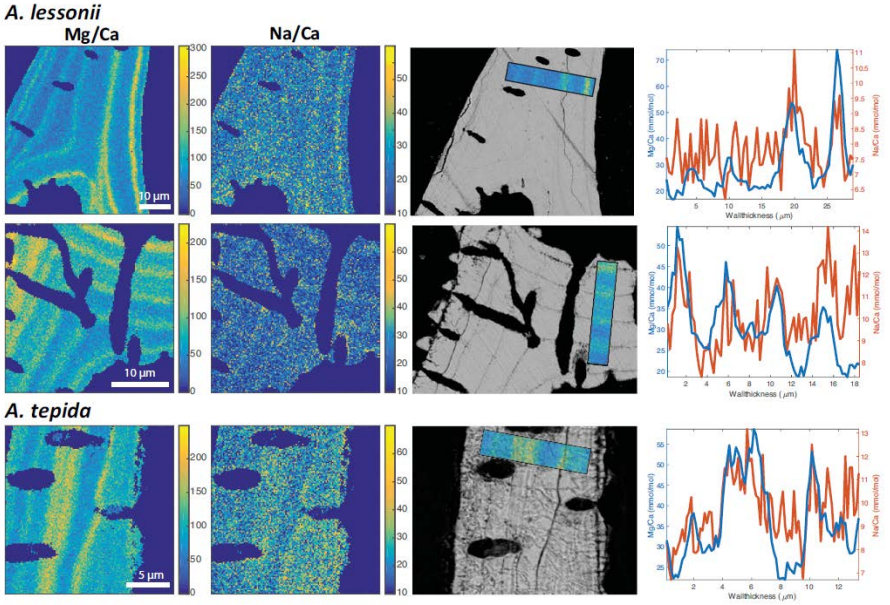

650

651 **Foraminiferal Mg/Ca_{cc} and Na/Ca_{cc} (left two panels) intensity ratio maps, obtained with EPMA, for three**
652 **specimens of *A. lessonii* grown at a salinity of 30 (upper panels), 25 (middle panels) and 40 (lower panels).**
653 **Right panels shows profiles for Mg/Ca (blue) and Na/Ca (red), based on averaged EPMA ratios scaled to**
654 **LA-ICP-MS measurements of the same specimens, of an averaged transact area through the chamber wall**
655 **perpendicular to the POS. The transect areas are indicated on top of backscatter SEM images, showing that**
656 **the high El/Ca bands overlap with the primary organic sheet (POS) and subsequent organic linings.**

657

658 **Appendix D.**

Biogeosciences Discuss., https://doi.org/10.5194/bg-2017-481
Manuscript under review for journal Biogeosciences
Discussion started: 11 December 2017

Orthogonal regression results

A. lessonii				*A. tepida*			
p-value (x,y)	r	Slope	y-Intercept	p-value (x,y)	r	Slope	y-Intercept
(Mg/Ca, Na/Ca)				**(Mg/Ca, Na/Ca)**			
p<0.001	0,71	0,21	2,21	p<0.001	0,35	1,64	1,63
p<0.001	0,52	0,17	3,89	p>0.05	0,24	2,14	0,41
p<0.001	0,57	0,17	4,06	p<0.001	0,62	0,86	3,14
p<0.001	0,89	0,14	5,44	p<0.001	0,53	1,19	2,35
p<0.001	0,69	0,16	5,12	p<0.001	0,84	1,34	1,89
(Mg/Ca, Sr/Ca)				**(Mg/Ca, Sr/Ca)**			
p<0.001	0,63	0,02	1,19	p<0.01	0,28	0,23	0,89
p<0.001	0,64	0,02	1,18	p>0.05	0,20	0,13	1,13
p<0.001	0,76	0,02	1,19	p>0.05	0,18	0,06	1,33
p<0.001	0,90	0,01	1,22	p>0.05	0,17	0,13	1,19
p<0.001	0,73	0,02	1,14	p>0.05	-0,28	-0,16	2,12
(Na/Ca, Sr/Ca)				**(Na/Ca, Sr/Ca)**			
p<0.001	0,58	0,09	1,00	p<0.01	0,29	0,14	0,66
p<0.001	0,47	0,10	0,78	p>0.05	0,10	0,06	1,10
p<0.001	0,72	0,10	0,77	p>0.05	0,23	0,07	1,10
p<0.001	0,94	0,11	0,62	p>0.05	0,18	0,11	0,94
p<0.001	0,80	0,12	0,53	p>0.05	-0,32	-0,12	2,34

Results for the orthogonal regressions testing the correlations between single-spot El^1/Ca and El^2/Ca, within each salinity conditions, for *A. lessonii* and *A. tepida*.

Appendix E.

Biogeosciences Discuss., https://doi.org/10.5194/bg-2017-481
Manuscript under review for journal Biogeosciences
Discussion started: 11 December 2017

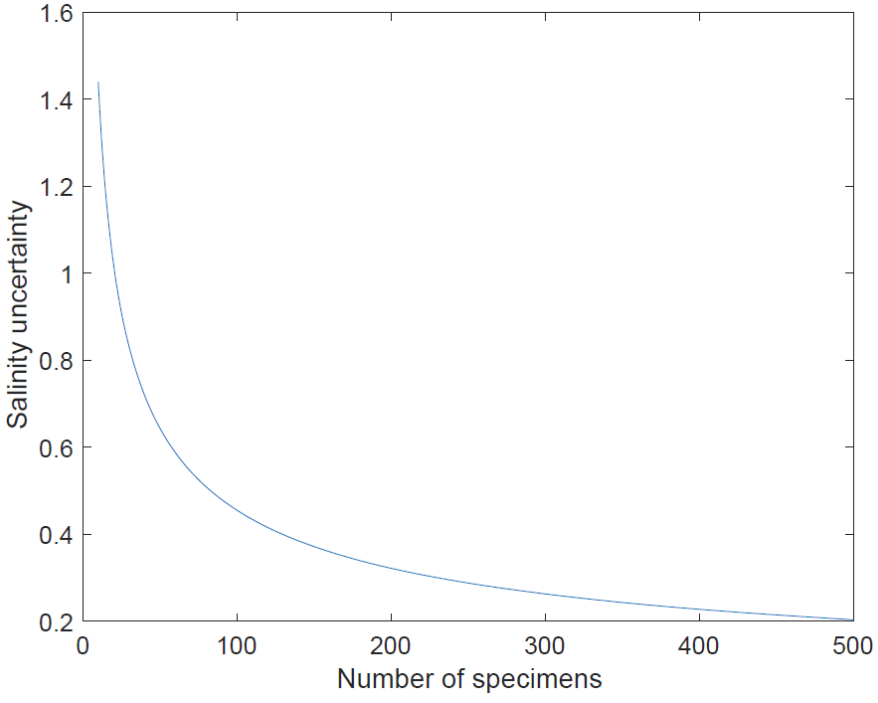

Figure showing the relationship between the salinity uncertainty and number of measured specimens for the Na/Ca_{cc} - salinity calibration of *A. lessonii*, calculated following Eq. (1):

$$\text{Salinity uncertainty} = (2 * \text{RSD} * \text{Number of specimens}^{-0.5}) / \text{Sensitivity} \quad (1)$$

Whereby sensitivity is the slope of the calibration.